

**Universitat de Lleida**

Document downloaded from:

<http://hdl.handle.net/10459.1/66697>

The final publication is available at:

<https://doi.org/10.1016/j.scitotenv.2019.06.121>

Copyright

cc-by-nc-nd, (c) Elsevier, 2019



Està subjecte a una llicència de [Reconeixement-NoComercial-SenseObraDerivada 3.0 de Creative Commons](https://creativecommons.org/licenses/by-nc-nd/3.0/)

1 **Assessment of spray drift potential reduction for hollow-cone**  
2 **nozzles: Part 1. Classification using indirect methods.**

3

4 Xavier Torrent<sup>a\*</sup>, Eduard Gregorio<sup>a</sup>, Jean-Paul Douzals<sup>b</sup>, Cyril Tinet<sup>b</sup>, Joan R. Rosell-Polo<sup>a</sup>,  
5 Santiago Planas<sup>a,c</sup>

6 <sup>a</sup> Research Group in AgroICT & Precision Agriculture, Department of Agricultural and Forest  
7 Engineering, Universitat de Lleida (UdL)-Agrotecnio Center, ETSEA, Av. Rovira Roure, 191,  
8 25198 Lleida, Spain.

9 <sup>b</sup> UMR ITAP, IRSTEA, Montpellier SupAgro, Université de Montpellier. 361 rue Jean-François  
10 Breton, BP 9505, F-34196 Montpellier Cedex, France.

11 <sup>c</sup> Plant Health Services. Generalitat de Catalunya, Avda. Rovira Roure, 191, 25198, Lleida, Spain.

12 \* Corresponding author. E-mail address: [xavier.torrent@eagrof.udl.cat](mailto:xavier.torrent@eagrof.udl.cat) (X. Torrent).

13

14 **Abstract**

15 Spray drift is one of the main pollution sources identified when pesticides are sprayed on crops.  
16 In this work, in order to simplify the evaluation of hollow-cone nozzles according to their drift  
17 potential reduction, several models commonly used were tested by three indirect methods: phase  
18 Doppler particle analyser (PDPA) and two different wind tunnels. The main aim of this study is  
19 then to classify for the first time these hollow-cone nozzle models all of them used in tree crop  
20 spraying (3D crops). A comparison between these indirect methods to assess their suitability and  
21 to provide guidelines for a spray drift classification of hollow-cone nozzles was carried out. The  
22 results show that, in general terms, all methods allow hollow-cone nozzle classifications  
23 according to their drift potential reduction (*DPR*) with a similar trend. Among all the parameters

24 determined with the PDPA, the  $V_{100}$  parameter performed best in differentiating the tested nozzles  
 25 among drift reduction classes. In the wind tunnel, similar values were obtained for both  
 26 sedimenting and airborne drift depositions. The  $V_{100}$  parameter displayed a high correlation (up  
 27 to  $R^2=0.948$ ) with the drift potential tested with the wind tunnel. It is concluded that in general,  
 28 the evaluated indirect methods provide equivalent classification results. Additional studies with a  
 29 greater variety of nozzle types are required to achieve a proposal of harmonized methodology for  
 30 testing hollow-cone nozzles.

31

32 **Keywords:** Pesticide, spray, drift, drift potential, droplet size, nozzle classification.

### 33 Nomenclature

34	$DP$	drift potential (%)
35	$DP_H$	sedimenting drift potential (%)
36	$DPR$	drift potential reduction (%)
37	$DPR_H$	drift potential reduction based on sedimenting deposition in wind tunnel (%)
38	$DPR_V$	drift potential reduction based on airborne deposition in wind tunnel (%)
39	$DPR_{D_{V_x}}$	drift potential reduction based on $D_{V_x}$ (%)
40	$DPR_{V_x}$	drift potential reduction based on $V_x$ (%)
41	$D_{V_x}$	volume diameter, indicating that the $x$ (% of spray volume) is in smaller
42		droplets ( $\mu\text{m}$ )
43	DRN	drift reduction nozzle
44	FF	flat-fan
45	FC	full-cone
46	HC	hollow-cone
47	PDPA	phase Doppler particle analyser
48	STN	standard nozzle
49	$V_x$	volume fraction of droplets smaller than $x$ $\mu\text{m}$ in diameter (%)

50	WT1	ISO wind tunnel
51	WT2	volumetric wind tunnel

52

### 53 **1. Introduction**

54 Spray drift is one of the main pollution sources identified when pesticides (also known as plant  
55 protection products, PPP) are applied on crops. Harmful effects of pesticides on humans and the  
56 environment are known for years. The potential adverse consequences of PPP usage can be  
57 significantly dispersed along time and space. As a result, the effects of pesticides on living beings,  
58 including humans, may emerge far away from the place where the treatment was performed and  
59 often after a long time. Field spray treatments can cause exposure to humans by several ways such  
60 as inhalation and dermal contact with the PPP spray drift during the application or with the PPP  
61 volatilised fraction some time after the treatment (Butler Ellis et al., 2010 and 2018; Damalas, C.  
62 A. 2015). The spray drift of PPP can be evaluated with a variety of methodologies. These can be  
63 divided into two types: those applied in field with the aim of measuring actual drift under real-  
64 life conditions (direct methods); and those which attempt to estimate drift potential (*DP*) under  
65 controlled conditions (indirect methods).

66 In field trials, the use of passive collectors continues to be the most popular methodology for the  
67 evaluation of drift during an application (McArtney and Obermiller, 2008; Garcerá et al., 2017;  
68 Torrent et al., 2017; Kasner et al., 2018), even though the process required is time-consuming and  
69 labour-intensive. Other authors, with the aim of simplifying the process, have developed spray  
70 drift models, based on many spray drift trials carried out in field conditions, to predict this  
71 phenomenon (Holterman et al., 2017). In recent years, the application of light detection and  
72 ranging (LiDAR) systems (Hiscox et al., 2006; Gregorio et al., 2014, 2016) for the field  
73 measurement of spray drift has been proposed. These systems have important advantages over  
74 passive collectors, both in terms of sensor performance (range and time-resolved measurements)  
75 and lower labour requirements.

76 The aim of the so-called indirect methods is to determine  $DP$ , defined as the fraction of the spray,  
77 as a percentage of the output of a spray generator, that is displaced downwind as airborne spray  
78 (ISO 22856:2008). The main advantage of indirect methods is their capacity to delimit the  
79 complexity and large number of variables that intervene in the drift phenomenon, as the tests are  
80 performed under controlled and reproducible conditions. Dimensional analyses of droplet  
81 populations are key to interpreting spray drift, with  $V_{100}$  the droplet size parameter most related  
82 to drift prone situations, as reported by Bouse et al. (1990) and Arvidsson et al. (2011). For this  
83 reason, numerous studies have been performed with characterisations of nozzle-generated droplet  
84 populations. In the vast majority of these studies, fan-type nozzles have been tested (Nuyttens et  
85 al., 2007), which are normally used in the treatment of field crops (2D crops). However, it is also  
86 of interest to evaluate hollow-cone nozzles. These are used in tree crop treatments (3D crops),  
87 where larger amounts of PPP tend to be used and where  $DP$  may be augmented because of the  
88 use of air-assistance in the treatment. One of the few studies to undertake a classification of this  
89 type of nozzle was that of Van de Zande et al. (2008), using a phase Doppler particle analyser  
90 (PDPA), as was also the case in subsequent studies by Holterman (2008, 2009). In these latter  
91 studies, an analysis was made of the effects of different variables (minimum number of droplets,  
92 scanning typology, nozzle height with respect to the measuring point) on droplet sizing. Good  
93 correlations have been found in comparative studies of different techniques (PDPA, laser  
94 diffraction analysis and particle/droplet imaging analysis (PDIA) (Herbst (2001a; b).

95 However, with so many techniques (phase Doppler particle analysis (Tuck et al., 1997), laser  
96 diffraction analysis (Derksen et al., 1999), particle measuring system (PMS) (Teske et al., 2000),  
97 and particle droplet imaging analysis (Kashdan et al., 2007)) available to characterise nozzle-  
98 generated droplet populations, the results can vary. In this sense, to harmonize the results obtained  
99 through the different methodologies, the ISO 25358:2018 proposes a methodology based on a set  
100 of standard nozzles for the definition of droplet size class boundaries.

101 The wind tunnel is currently the most commonly used indirect method to study and classify  
102 nozzles according to their  $DP$ . Following this method, Taylor et al. (2004) determined the  $DP$  of

103 ASAE reference nozzles for different wind speeds and nozzle heights. Guler et al. (2006, 2007)  
104 and Ferguson et al. (2015, 2016) evaluated drift potential reduction (*DPR*), comparing standard  
105 and drift reduction flat-fan nozzles. In addition to the effect of nozzle type, evaluation has also  
106 been made of the effect of nozzle size (Nuyttens et al., 2009). Studies have also been made of the  
107 correlation between wind tunnel recorded data and field measured data in order to extrapolate the  
108 drift reduction values to field conditions (Butler Ellis et al., 2017; Torrent et al., 2017). Douzals  
109 et al. (2016, 2018) measured droplet size in a wind tunnel using different flat-fan nozzles, heights,  
110 orientations and wind speeds, defining new *DP* indicators such as drift ratio (DR) and time-of-  
111 flight (ToF). Another methodology to evaluate *DP* for different operating conditions is based on  
112 the use of a test bench (Balsari et al., 2007), which allows assessment of working parameters  
113 (Miranda-Fuentes et al., 2018) and classification of different application equipment according to  
114 their potential drift reduction (Gil et al., 2014; Grella et al., 2019).

115 Most of the previously cited studies reporting indirect drift assessments focused on flat-fan  
116 nozzles, being these the most used in field crops. The amount of spray drift generated by hollow-  
117 cone nozzles used in tree crops is significantly higher. Therefore, the main aim of the present  
118 study is to classify for the first time hollow-cone nozzles used in tree crops (3D crops). A second  
119 objective is to compare three indirect methodologies for *DPR* determination: PDPA, ISO wind  
120 tunnel (WT1) (discrete collection) and volumetric wind tunnel (WT2) (whole collection) to  
121 provide guidelines for drafting a harmonized methodology for testing hollow-cone nozzles.

## 122 **2. Materials and methods**

### 123 *2.1. Droplet size characterization using a PDPA*

124 The droplet size spectrum was characterized using a phase Doppler particle analyser device  
125 (PDPA, Dantec Dynamics A/S. Skovlunde, Denmark) at the Information and Technologies for  
126 Agricultural Processes Joint Research Unit (IRSTEA, Montpellier, France). A total of 16 nozzles  
127 were tested, including 12 hollow-cone types (HC), of which 7 were standard STN and 5 drift  
128 reduction (DRN models, 3 flat-fan (FF) and 1 full-cone (FC). The models of the hollow cone

129 chose are the most used for spraying tree crops in Spain. The FF nozzles tested as threshold  
130 nozzles were the previously established by Van de Zande et al. (2008) in their HC classification,  
131 while the FC was an example of a cone nozzle used in citrus crops. The set of nozzles tested  
132 allowed a study to be made of nozzle type and size. The tested nozzle models and types are shown  
133 in Table 1, as well as the working pressure at which the measurements were taken, the flow rate  
134 and the measuring height of the PDPA. The nozzles correspond to different models of the Albus  
135 ATR, TVI and AVI series (Solcera, Evreux, France), Lechler ID (Lechler GmbH,  
136 Metzingen, Germany), and TeeJet DG (Spraying Systems Co. Wheaton, IL, USA).

**Table 1.** Nozzles characterized with the PDPA.

Nozzle		Pressure (kPa)	Nominal flow rate (L min <sup>-1</sup> )	PDPA measurement point height (m)
Model	Type			
ATR 80 Lilac *		700	0.42	
ATR 80 Brown		700	0.56	
ATR 80 Yellow		700	0.86	
ATR 80 Orange	HC-STN	700	1.17	0.15
ATR 80 Red		700	1.62	
ATR 80 Grey		700/1000	1.76/2.08	
ATR 80 Green		700	2.00	
TVI 8001 Orange		700	0.61	
TVI 80015 Green		700	0.92	
TVI 8002 Yellow	HC-DRN	700	1.22	0.15
TVI 80025 Purple		700	1.53	
TVI 8003 Blue		700/1000	1.83/2.19	
AVI 80015 Green	FF-DRN	700	0.92	0.30
ID 9001C Orange		500	0.51	
DG 8002 Yellow	FF-STN	700	1.21	0.30
D3DC35 Brown	FC-STN	1000	2.00	0.15

138 *HC-STN: Hollow-cone standard nozzle; HC-DRN: Hollow-cone drift reduction nozzle; FC-STN: Full-cone standard nozzle; FF-STN:*  
139 *Flat-fan standard nozzle; FF-DRN: Flat-fan drift reduction nozzle. \* Reference nozzle.*

140 The flow rate of ten nozzles of each model was measured, and the nozzle which most closely  
141 approximated the nominal flow rate (with a deviation from the nominal flow rate in all cases  
142 below 5%) was the one chosen for testing. When coinciding, the same units of the nozzle models  
143 selected in this case were also used in the WT1 and WT2 tests (see sections 2.2 and 2.3).

144 Tap water was used as spray liquid for all nozzles. The temperature of the spray liquid was 20±1°C  
145 and the liquid pressure was 500, 700 or 1000 kPa depending on the nozzle model tested (Table  
146 1). All measurements were performed in an air conditioned room at 20±1°C at 70-80% of relative  
147 humidity. Three repetitions for each nozzle model were carried out. Each repetition was  
148 performed with a different single nozzle unit, so three different units were tested for each model.

149 In all tests, the nozzle position was 0.15 m above the measuring point for all hollow-cone nozzles  
150 and 0.30 m for the flat-fan nozzles due to the fan length. To sample the whole cone section, the



151 scan trajectory for the hollow-cone nozzles consisted of a continuous scan of the spray along 7  
 152 parallel lines 300 mm long with a separation of 36 mm (Fig. 1a). In the case of the FF-type  
 153 nozzles, line length was 800 mm and line separation 15 mm (Fig. 1b). All measurements were  
 154 carried out along the long axis of the spray cloud with a linear displacement of the nozzle at a  
 155 constant speed of  $3 \text{ mm s}^{-1}$  during 780 s and 1860 s for the cone-type and FF-type nozzles,  
 156 respectively.

157 Measurement acquisition was performed with the software BSA Flow v.4.50 (PDPA, Dantec  
 158 Dynamics A/S, Skovlunde, Denmark) and only spherical droplets were considered (the  
 159 percentage of non-spherical droplets was below 10% for all tested nozzles). For each nozzle  
 160 several parameters were determined from the cumulative volumetric droplet size distribution and  
 161 the following percentile characteristics calculated: i)  $D_{V10}$ ,  $D_{V50}$ , and  $D_{V90}$ , representing the  
 162 diameter below which smaller droplets constitute 10%, 50% and 90% of the total volume,  
 163 respectively; and ii) the proportional characteristics  $V_{100}$  and  $V_{200}$ , representing the percentage of  
 164 volume of drops having a diameter smaller than  $100 \mu\text{m}$  and  $200 \mu\text{m}$ , respectively.

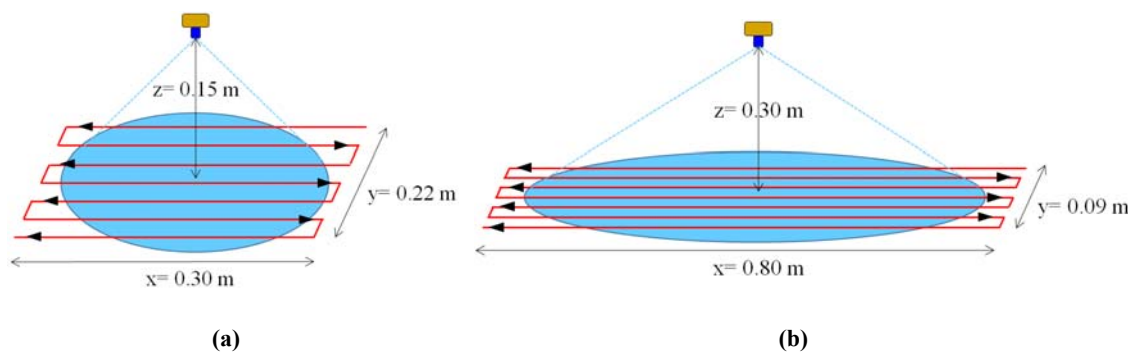


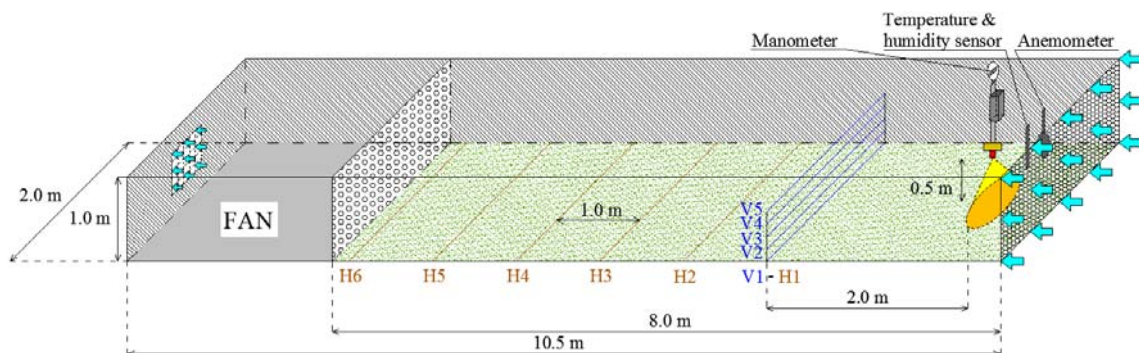
**Fig. 1.** Scanning path during PDPA droplet size characterization corresponding to the following nozzles: (a) HC-STN, FC-STN and HC-DRN; (b) FF-STN and FF-DRN.

165

166 2.2. ISO wind tunnel (WT1) tests

167 A detailed explanation is provided in this section of the methodology employed in the WT1 wind  
 168 tunnel, situated in Maqcentre - Parc Científic i Tecnològic Agroalimentari de Lleida (PCiTAL,  
 169 Lleida, Spain). The tunnel characteristics meet those of the International Standard ISO  
 170 22856:2008. The tunnel is 2.0 m wide, 1.0 m high and has an operating length of 7.0 m (Fig. 2).  
 171 Test conditions in the tunnel interior were  $2\pm 0.1 \text{ m s}^{-1}$  for air flow, with turbulences below 8%,  
 172 and local speed variations below 5%.

173 A total of 38 nozzles were tested of different manufacturers: 19 HC-STN nozzles, 9 HC-DRN  
 174 nozzles, 1 FC-STN nozzle, 6 FF-STN nozzles and 3 FF-DRN nozzles. Included in this list are the  
 175 28 most representative nozzle models and sizes used on tree crops in Spain. Ten additional nozzles  
 176 used on field crops were also included to enable comparison with tests made in other laboratories.  
 177 Test pressure for the HC nozzles was 500, 700 and 1000 kPa, for the FC nozzle was 1000 kPa  
 178 and for the FF nozzles 200, 250, 300, 500 and 700 kPa depending on the nozzle tested (Table 2).  
 179 In all tests, a mixture of a water-soluble fluorescent tracer, brilliant sulfoflavine (BSF) yellow (CI  
 180 56205) (Biovalley, Marne La Vallee, France), was sprayed at a concentration of  $0.3 \text{ g L}^{-1}$ , with a  
 181 total of 3 repetitions per tested nozzle, following the methodology described by Torrent et al.  
 182 (2017).



183  
 184 **Fig. 2.** Inside view setup of the WT1. Dimensions and position of the collectors (horizontals: H1-H6, verticals: V1-  
 185 V5). Figure adapted from Torrent et al. (2017).  
 186

**Table 2.** Nozzles tested using WT1.

Nozzle			Pressure	Flow rate
Manufacturer	Model	Type	(kPa)	(L min <sup>-1</sup> )
Abba	AG 1030.015 Green		700	0.92
	AG 1030.02 Yellow	HC-STN	700	1.22
	AG 1030.025 Lilac		700	1.53
Agrotop	Air Mix HC 80.025 Lilac	FF-DRN	500	0.60
Albuz	ATI 60.015 Green		700	0.92
	ATI 60.025 Lilac		700	1.53
	ATR 60 Red		700	1.62
	ATR 60 Yellow		700	0.86
	ATR 80 Grey	HC-STN	1000	2.08
	ATR 80 Lilac*		700	0.42
	ATR 80 Orange		700	1.17
	ATR 80 Red		700	1.62
	ATR 80 Yellow		700	0.86
	AVI 80015 Green	FF-DRN	700	0.92
	TVI 80015 Green		700	0.92
	TVI 8002 Yellow	HC-DRN	700	1.22
	TVI 80025 Purple		700	1.53
TVI 8003 Blue		1000	2.19	
Hardi	1553-14	HC-STN	1000	0.60
	1553-18		1000	1.10
	F110.03 Blue	FF-STN	300	1.20
Lechler	ID 9001C Orange	FF-DRN	500/700	0.51/0.60
	ITR 8001 Orange		700	0.60
	ITR 80015 Green	HC-DRN	700	0.90
	ITR 8002 Yellow		700	1.22
	LU 120.06 Grey	FF-STN	700	0.60
	TR 80015 Green		700	0.90
	TR 8002 Yellow	HC-STN	700	1.22
	TR 8003 Blue		700	1.81
Lurmark	F11003 Blue	FF-STN	300	1.18
	HCX 10 Black	HC-STN	500	0.86
	HCX 12 Yellow		500	1.03
Teejet	D3DC35 Brown	FC-STN	1000	2.00

DG 8002 Yellow	FF-STN	700	1.21
TXA 8002 VK Yellow		700	1.20
TXA 8003 VK Blue	HC-DRN	700	1.80
XR 8008 VK White		250	2.88
XR 8015 (Steel)	FF-STN	200	4.90

188 *HC-STN: Hollow-cone standard nozzle; HC-DRN: Hollow-cone drift reduction nozzle; FC-STN:*  
 189 *Full-cone standard nozzle; FF-STN: Flat-fan standard nozzle; FF-AIN: Flat-fan air induction*  
 190 *nozzle. \* Reference nozzle.*

191

### 192 2.3. Volumetric wind tunnel (WT2) tests

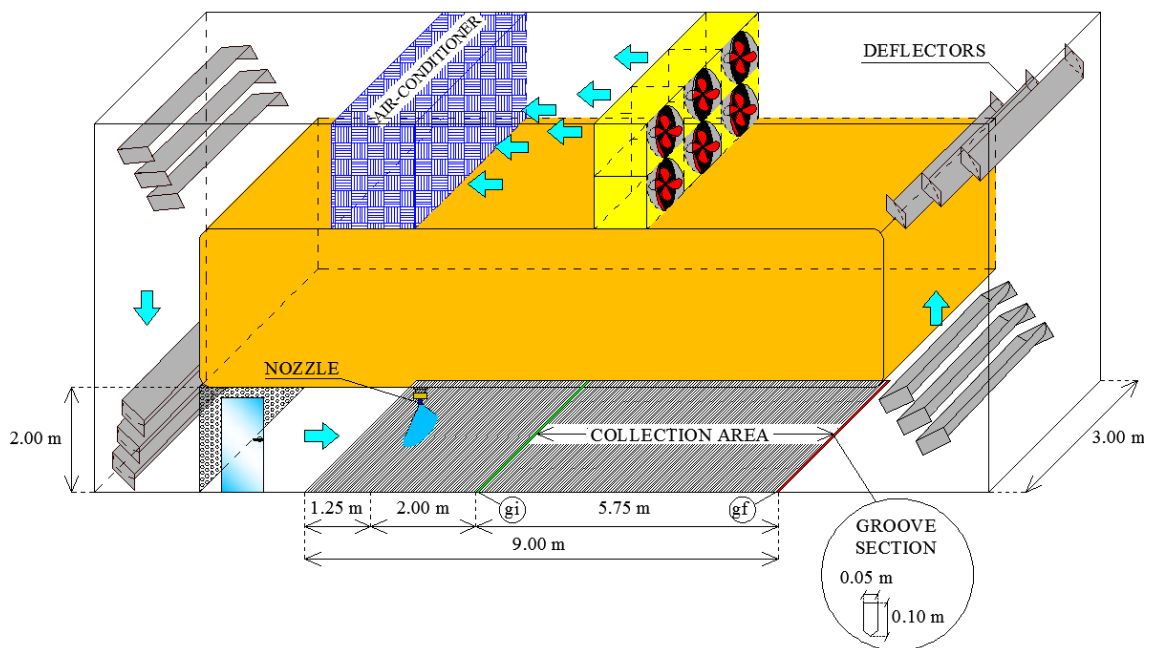
193 The WT2 tunnel is located at the facilities of the Information & Technologies for Agricultural  
 194 Processes Joint Research Unit (IRSTEA, Montpellier, France). This tunnel was designed based  
 195 on a criterion different to ISO 22856:2008. The tunnel is 3.0 m wide, 2.0 m high and has an  
 196 operating length of 9.0 m, with a total of 180 grooves along the floor of the tunnel which are 50  
 197 mm wide and 100 mm deep (Fig. 3). The fluid is collected using 60 collecting tubes, making it  
 198 necessary to position the set of tubes in three consecutive sections to cover the whole tunnel. The  
 199 tunnel is comprised of a closed circuit in which air flow is generated by 6 air fans. Air temperature  
 200 and humidity are automatically controlled. The most important distinguishing feature of the WT2  
 201 tunnel is that, unlike the WT1 tunnel that uses droplet collectors to determine sedimenting and  
 202 airborne drift, a distribution test bench composed of slightly inclined grooved channels are  
 203 situated on the tunnel floor to collect the sedimented droplets. The liquid deposited in each groove  
 204 travels towards a measuring tube system where the flow of each groove is measured individually  
 205 using load cells (Douzals and Al Heidary, 2014).

206 The sprayed fluid was tap water at a temperature of  $20\pm 1^\circ\text{C}$ . Ambient conditions in the tunnel  
 207 interior were  $20\pm 1^\circ\text{C}$  and 70-80% relative humidity. Air flow speed was  $2.0\pm 0.1\text{ m}\cdot\text{s}^{-1}$ .

208 The selected nozzle units were those whose flow rate closest to the nominal, as explained in  
 209 section 2.1. As can be seen in Table 3, a total of 4 Albus hollow cone nozzles were tested, two of  
 210 which were STN type (ATR 80 Lilac and ATR 80 Grey) and two DRN (TVI 80025 Purple and

211 TVI 8003 Blue), at a pressure of 700 kPa. The ATR 80 Grey and TVI 8003 nozzles were also  
 212 tested at 1000 kPa to facilitate a comparison with the WT1 tests. Pressure was set with a 5 kPa  
 213 precision and automatically corrected with a frequency of 3 Hz.

214 Each nozzle was tested in both vertical position, as in the WT1 (position for field crops), and in  
 215 horizontal position (position for tree crops). The nozzles were situated 1.25 m from the start of  
 216 the collection area. As shown in Fig. 2, the collection area considered for deposition evaluation  
 217 was between grooves  $g_i$  and  $g_f$ , positioned at 2.00 m and 7.70 m downwind from the tested nozzle,  
 218 respectively. In addition, tests were conducted with the ATR 80 Grey and TVI 8003 Blue nozzles  
 219 spraying vertically and horizontally, using two units at the same time situated on a bar and  
 220 separated from each other by a distance of 1.50 m.



221

222

**Fig. 3.** Inside view setup of the WT2. Dimensions, nozzle and collection area positions.

223

224

**Table 3.** Nozzles tested using WT2.

Nozzle		Pressure	Flow rate	VS-1N	HS-1N	VS-2N	HS-2N
Model	Type	(kPa)	(L min <sup>-1</sup> )				
ATR 80 Lilac *	HC-STN	700	0.42	X	X	-	-
ATR 80 Grey		700/1000	1.76/2.08	X	X	X	X
TVI 80025 Purple	HC-DRN	700	1.53	X	X	-	-
TVI 8003 Blue		700/1000	1.83/2.19	X	X	X/-	X

225

*HC-STN: Hollow-cone standard nozzle; HC-DRN: Hollow-cone drift reduction nozzle*

226

*VS-1N: Vertical spraying with 1 nozzle; HS-1N: Horizontal spraying with 1 nozzle; VS-2N: Vertical spraying with 2 nozzles; HS-2N:*

227

*Horizontal spraying with 2 nozzles. \* Reference nozzle.*

228

229 

#### 2.4. Data analysis

230

Details are provided in this section of the post-processing of the results obtained for each of the

231

test methodologies (PDPA, WT1 and WT2).

232

232 

##### 2.4.1. Statistical analysis

233

For the case in which a comparative analysis was made of the PDPA, WT1 and WT2

234

methodologies, the results shown in the tables and figures correspond to the mean value of the 3

235

replicate tests made in each case.

236

To study the effect of nozzle type, size and working pressure from the results obtained, a one-way

237

analysis of variance (ANOVA) with Fisher's least significant difference (LSD) test was performed

238

for each effect. Previously, the normality and homogeneity of variance of the studied variables

239

were verified with the Shapiro-Wilk test and Levene's test, respectively. A confidence level of

240

95% was considered in all tests. Statistical analyses were done using JMP® Pro 13 (SAS Institute

241

Inc., Cary, NC, 1989-2007 for Windows).

242 2.4.2. Spray drift potential reduction

243 In the first methodology tested, droplet size characterisation using PDPA, the characteristic  
244 parameters  $D_{V50}$ ,  $V_{100}$  and  $V_{200}$  were used as  $DP$  indicators.

245 For the case of WT1, the  $DP$  of each nozzle was calculated in accordance with ISO 22856:2008,  
246 based on the following expressions:

$$247 \quad DP_V(WT1) = \sum_{i=1}^5 V_{T(i)} \quad (1)$$

$$248 \quad DP_H(WT1) = \sum_{j=1}^6 H_{T(j)} \quad (2)$$

249 where  $DP_V(WT1)$  and  $DP_H(WT1)$  represent the total airborne and the total sedimenting  $DP$  for the  
250 WT1, respectively.  $V_{T(i)}$  is the airborne  $DP$  at the vertical collector line  $i$  (%) (there were 5 vertical  
251 collector lines); while  $H_{T(j)}$  is the sedimenting  $DP$  at the collector line  $j$  (%) (there were 6  
252 horizontal collector lines), according to the following expressions:

$$253 \quad V_{T(i)} \text{ or } H_{T(j)} = \left( \frac{v_{(i/j)} \cdot \frac{d_C}{D_C}}{q_N \cdot (t_S/60)} \right) \cdot 100 \quad (3)$$

254 where:  $v_{(i/j)}$  is the volume deposited in the collector line  $i$  or  $j$  (L), given by Eq. (4);  $d_C$ , the distance  
255 between collectors (0.1 m for vertical collectors and 1.0 m for horizontal collectors);  $D_C$ , the  
256 collector diameter (0.002 m);  $q_N$ , the nozzle flow rate (L min<sup>-1</sup>); and  $t_S$ , the spraying time (s).

$$257 \quad v_{(i/j)} = \frac{v_D \cdot F}{C_D \cdot 10^6} \quad (4)$$

258 where:  $v_D$  is the sample dilution volume (L);  $F$ , the fluorimeter reading ( $\mu\text{g BSF L}^{-1}$ ); and  $C_D$ , the  
259 BSF concentration ( $\text{g BSF L}^{-1}$ ).

260 For the case of WT2, only the  $DP_H$  was determined. This was calculated as the global fraction of  
261 the sprayed liquid transported by the grooved channels along the tunnel, from a distance 2.00 m  
262 downwind from the nozzle position to 7.70 m. Finally,  $DP_H$  was calculated using the following  
263 expression:

$$264 \quad DP_H(WT2) = \sum_{g=gi}^{gf} H_{T(g)} \quad (5)$$

265 where:  $gi$  and  $gf$  are the grooves at 2.00 and 7.70 m downwind from the tested nozzle, respectively;

266 and  $H_{T(g)}$  is the sedimenting spray mass at groove  $g$  (%), according to the following expression:

$$267 \quad H_{T(g)} = \frac{W \cdot 60}{t_C \cdot q_N} \quad (6)$$

268 where:  $W$  is the collected liquid mass (kg);  $t_C$  is the collection time (s); and  $q_N$  is the nozzle flow

269 rate ( $L \text{ min}^{-1}$ ).

270 From the corresponding  $DP$  values obtained for each methodology and nozzle, the  $DPR$  was then

271 calculated. The  $DPR$  was determined by relating the value of the  $DP$  of the candidate nozzle (C)

272 with the  $DP$  value of the reference nozzle (R), in all cases the Albus ATR 80 Lilac at 700 kPa,

273 using the following expression:

$$274 \quad DPR = (1 - (DP_C/DP_R)) \cdot 100 \quad (7)$$

275 where:  $DP_C$  is the drift potential of the candidate nozzle (%); and  $DP_R$  is the drift potential of the

276 reference nozzle (%).

277

### 278 **3. Results**

#### 279 *3.1. Droplet size characterization using a PDPA*

280 Table 4 shows the characteristic parameters of the droplet population ( $D_{V10}$ ,  $D_{V50}$ ,  $D_{V90}$ ,  $V_{100}$ ,  $V_{200}$ )

281 obtained with the PDPA. As expected, the DRN nozzles produced larger droplets than the STN

282 nozzles.



283 **Table 4.** Droplet size spectrum characteristics of the tested nozzles arranged according to the  $V_{100}$  value.

Nozzle		Pressure	$D_{V10}$	$D_{V50}$	$D_{V90}$	$V_{100}$	$V_{200}$
Model	Type	(kPa)	( $\mu\text{m}$ )	( $\mu\text{m}$ )	( $\mu\text{m}$ )	(%)	(%)
ATR 80 Lilac *	HC-STN	700	57.20	95.30	144.10	54.87	99.06
ATR 80 Brown	HC-STN	700	61.70	105.93	158.10	44.34	97.66
ATR 80 Yellow	HC-STN	700	62.30	113.93	181.40	38.10	93.56
D3DC35 Brown	FC-STN	1000	68.47	126.63	237.30	30.19	83.66
ATR 80 Orange	HC-STN	700	67.90	125.37	196.47	29.99	90.80
ATR 80 Grey	HC-STN	1000	70.93	132.87	219.40	26.16	85.80
ATR 80 Red	HC-STN	700	74.33	139.00	226.33	23.01	83.30
ATR 80 Grey	HC-STN	700	75.17	144.20	240.80	21.91	79.40
ATR 80 Green	HC-STN	700	79.27	151.50	253.97	18.97	75.71
DG 8002 Yellow	FF-STN	700	105.27	222.10	408.33	8.72	41.25
AVI 80015 Green	FF-DRN	700	190.23	414.37	853.90	1.44	11.54
ID 9001C Orange	FF-DRN	500	287.87	589.63	842.43	0.34	3.30
TVI 8003 Blue	HC-DRN	700	264.23	489.47	792.47	0.32	3.86
TVI 8003 Blue	HC-DRN	1000	281.50	514.47	809.97	0.27	3.11
TVI 8001 Orange	HC-DRN	700	279.33	552.57	841.47	0.25	3.43
TVI 80015 Green	HC-DRN	700	273.03	513.63	821.03	0.25	3.38
TVI 8002 Yellow	HC-DRN	700	287.60	534.47	813.20	0.24	2.94
TVI 80025 Purple	HC-DRN	700	300.83	549.17	811.80	0.18	2.42

284 *HC-STN: Hollow-cone standard nozzle; HC-DRN: Hollow-cone drift reduction nozzle; FC-STN: Full-cone standard nozzle; FF-STN:*  
 285 *Flat-fan standard nozzle; FF-DRN: Flat-fan drift reduction nozzle. \* Reference nozzle.*

286 When considering the  $V_{100}$  values (Table 4), significant differences were found between Albu  
 287 STN and DRN nozzles of similar flow rate (ATR 80 Yellow-TVI 80015 Green, ATR 80 Orange-  
 288 TVI 8002 Yellow and ATR 80 Red-TVI 80025 Purple at 700 kPa; ATR 80 Grey-TVI 8003 Blue  
 289 at 1000 kPa). Also, as nozzle size increased, the  $V_{100}$  value decreased for the STN nozzles and  
 290 significant differences between different sizes were observed (ATR 80 Lilac-ATR 80 Yellow-  
 291 ATR 80 Orange-ATR 80 Red at 700 kPa). However, no significant differences between nozzle  
 292 size were observed for the DRN nozzles, with a  $V_{100}$  value even being obtained with the largest  
 293 tested hollow-cone nozzle size (TVI 8003 Blue) which was higher than the other values. A similar  
 294 trend was observed in the  $V_{200}$ ,  $D_{V10}$ ,  $D_{V50}$  and  $D_{V90}$  parameters.

295

296 The effect of pressure was analysed for an STN (ATR 80 Grey) and DRN (TVI 8003 Blue) nozzle,  
297 at 700 and 1000 kPa. In the case of the STN, significantly higher  $V_{100}$  and  $V_{200}$  values, and lower  
298 droplet size values, were obtained at 1000 kPa. In contrast, no significant differences were  
299 observed in any of the characteristic parameters for the DRN nozzle.

300

301 Table 5 shows the *DPR* results calculated on the basis of the  $V_{100}$ ,  $V_{200}$  and  $D_{V50}$  parameters. Nozzle  
302 classification was established based on the  $DPR_{V100}$  according to ISO 22369-1:2006. Threshold  
303 nozzles corresponding to 25%, 50%, 75%, 95% and 99% drift reduction classes are ATR 80  
304 Yellow, ATR 80 Grey at 1000 kPa, DG 8002 Yellow at 700 kPa, AVI 80015 Green at 700 kPa  
305 and ID 9001C Orange, respectively. For the  $V_{100}$  parameter, it can be seen how all the DRN  
306 models are classified in the same drift reduction class of 99%, except for AVI 80015 Green. The  
307 *DPR* values determined based on  $V_{200}$  and  $D_{V50}$  are lower than those calculated with the  $V_{100}$ , with  
308 lower spray drift reduction classes being obtained.

309 **Table 5.** *DPR* values of the tested nozzles based on three droplet size indicators ( $V_{100}$ ,  $V_{200}$  and  $D_{V50}$ ). Albus ATR 80  
 310 Lilac is considered the reference nozzle. The threshold nozzles for drift reduction classes are in bold. The position  
 311 number of each nozzle is given in brackets. Classification changes when considering  $DPR_{V200}$  or  $DPR_{DV50}$  instead of  
 312  $DPR_{V100}$  are highlighted in grey.

Nozzle		Pressure	$DPR_{V100}$	$DPR_{V200}$	$DPR_{DV50}$	Spray drift
Model	Type	(kPa)	(%)	(%)	(%)	reduction class
ATR 80 Lilac	HC-STN	700	0 (1)	0 (1)	0.00 (1)	Reference
ATR 80 Brown	HC-STN	700	19.18 (2)	1.41 (2)	10.04 (2)	<25%
<b>ATR 80 Yellow</b>	<b>HC-STN</b>	<b>700</b>	<b>30.55 (3)</b>	<b>5.55 (3)</b>	<b>16.35 (3)</b>	
D3DC35 Brown	FC-STN	1000	44.97 (4)	15.55 (6)	24.74 (5)	25%
ATR 80 Orange	HC-STN	700	45.34 (5)	8.34 (4)	23.98 (4)	
<b>ATR 80 Grey<sup>(a)</sup></b>	<b>HC-STN</b>	<b>1000</b>	<b>52.32 (6)</b>	<b>13.39 (5)</b>	<b>28.27 (6)</b>	
ATR 80 Red	HC-STN	700	58.06 (7)	15.91 (7)	31.44 (7)	50%
ATR 80 Grey	HC-STN	700	60.07 (8)	19.85 (8)	33.91 (8)	
ATR 80 Green	HC-STN	700	65.43 (9)	23.57 (9)	37.10 (9)	
<b>DG 8002 Yellow<sup>(b)</sup></b>	<b>FF-STN</b>	<b>700</b>	<b>84.11 (10)</b>	<b>58.36 (10)</b>	<b>57.09 (10)</b>	75%
<b>AVI 80015 Green<sup>(c)</sup></b>	<b>FF-DRN</b>	<b>700</b>	<b>97.37 (11)</b>	<b>88.35 (11)</b>	<b>77.00 (11)</b>	95%
<b>ID 9001C Orange<sup>(d)</sup></b>	<b>FF-DRN</b>	<b>500</b>	<b>99.39 (12)</b>	<b>96.66 (15)</b>	<b>83.84 (18)</b>	
TVI 8003 Blue	HC-DRN	700	99.41 (13)	96.10 (12)	80.53 (12)	
TVI 8003 Blue	HC-DRN	1000	99.51 (14)	96.86 (16)	81.48 (14)	
TVI 80015 Green	HC-DRN	700	99.54 (15)	96.59 (14)	81.45 (13)	99%
TVI 8001 Orange	HC-DRN	700	99.54 (16)	96.54 (13)	82.75 (17)	
TVI 8002 Yellow	HC-DRN	700	99.56 (17)	97.03 (17)	82.17 (15)	
TVI 80025 Purple	HC-DRN	700	99.68 (18)	97.55 (18)	82.65 (16)	

313 <sup>a, b, c, d</sup> Threshold nozzles corresponding to 25%, 50%, 75%, 95% and 99% drift reduction classes, respectively.

314 *HC-STN*: Hollow-cone standard nozzle; *HC-DRN*: Hollow-cone drift reduction nozzle; *FC-STN*: Full-cone standard nozzle; *FF-STN*:  
 315 Flat-fan standard nozzle; *FF-DRN*: Flat-fan drift reduction nozzle.

316

### 317 3.2. ISO wind tunnel (WTI) tests

318 Table 6 shows the results obtained in sedimenting and airborne drift potential reduction ( $DPR_H$   
 319 and  $DPR_V$ , respectively) for the 38 tested nozzles. Using these results, a classification of the  
 320 nozzles was made based on the  $DPR_H$ , determining their spray drift reduction class according to  
 321 the thresholds of 25%, 50%, 75%, 90% and 95% (Table 6). In general, it can be seen that the

322  $DPR_H$  and  $DPR_V$  values are similar for a specific nozzle, with similar classifications obtained for  
 323 both parameters. It can also be seen that, for nozzles with a reduction greater than 90%, the  $DPR_H$   
 324 takes slightly higher values than the  $DPR_V$ .

325

326 **Table 6.**  $DPR$  values of the tested nozzles determined from WT1 measurements. Albuz ATR 80 Lilac is considered  
 327 the reference nozzle. The threshold nozzles for drift reduction classes are in bold. The position number of each nozzle  
 328 is given in brackets. Classification changes when considering  $DPR_V$  instead of  $DPR_H$  are highlighted in grey.

329

Nozzle		Pressure	$DPR_H$	$DPR_V$	Spray drift
Model	Type	(kPa)	(%)	(%)	reduction class
ATR 80 Lilac	HC-STN	700	0 (1)	0 (1)	Reference
<b>1553-14</b>	<b>HC-STN</b>	<b>1000</b>	<b>9.5 (2)</b>	<b>39.49 (5)</b>	<25%
<b>ATR 60 Yellow</b>	<b>HC-STN</b>	<b>700</b>	<b>27.73 (3)</b>	<b>36.83 (3)</b>	
TR 80015 Green	HC-STN	700	31.34 (4)	35.14 (2)	
TXA 8002 VK Yellow	HC-DRN	700	32.18 (5)	39.43 (4)	
1553-18	HC-STN	1000	39.23 (6)	53.08 (9)	25%
AG 1030.015 Green	HC-STN	700	41.91 (7)	58.81 (11)	
HCX 10 Black	HC-STN	500	46.06 (8)	49.41 (7)	
HCX 12 Yellow	HC-STN	500	46.43 (9)	46.76 (6)	
<b>TR 8002 Yellow<sup>(a)</sup></b>	<b>HC-STN</b>	<b>700</b>	<b>53.1 (10)</b>	<b>52.17 (8)</b>	
ATI 60015 Green	HC-STN	700	55.1 (11)	60.04 (13)	
LU 12006 Grey	FF-STN	200	57.92 (12)	59.19 (12)	
TXA 8003 Blue	HC-DRN	700	60.44 (13)	58.55 (10)	
ATR 80 Yellow	HC-STN	700	63.56 (14)	66.45 (14)	
AG 1030.02 Yellow	HC-STN	700	67.76 (15)	69.50 (16)	50%
DG 8002 Yellow	FF-STN	700	70.60 (16)	67.32 (15)	
F11003 Blue	FF-STN	300	71.47 (17)	77.72 (22)	
ATR 80 Orange	HC-STN	700	71.5 (18)	70.95 (17)	
TR 8003 Blue	HC-STN	700	74.34 (19)	73.18 (18)	
F11003 Blue	FF-STN	300	74.96 (20)	76.39 (21)	
<b>ATR 60 Red<sup>(b)</sup></b>	<b>HC-STN</b>	<b>700</b>	<b>75.81 (21)</b>	<b>74.68 (19)</b>	
AG 1030.025 Lilac	HC-STN	700	78.67 (22)	75.57 (20)	75%
Air Mix HC 80025 Lilac	FF-DRN	500	85.68 (23)	86.62 (25)	
ATR 80 Red	HC-STN	700	87.77 (24)	81.96 (23)	

ID 9001C Orange	FF-DRN	700	88.60 (25)	88.74 (27)	
AVI 80015 Green	FF-DRN	700	88.80 (26)	89.98 (28)	
<b>ATR 80 Grey<sup>(c)</sup></b>	<b>HC-STN</b>	<b>1000</b>	<b>90.25 (27)</b>	<b>82.24 (24)</b>	
ATI 60025 Lilac	HC-STN	700	90.86 (28)	86.81 (26)	
ID 9001C Orange	FF-DRN	500	93.58 (29)	93.23 (30)	90%
D3DC35 Brown	FC-STN	1000	94.46 (30)	91.16 (29)	
TVI 8002 Yellow	HC-DRN	700	94.63 (31)	93.96 (32)	
<b>XR 8008 White<sup>(d)</sup></b>	<b>FF-STN</b>	<b>250</b>	<b>95.11 (32)</b>	<b>93.84 (31)</b>	
ITR 8001 Orange	HC-DRN	700	95.52 (33)	95.13 (33)	
TVI 80015 Green	HC-DRN	700	95.71 (34)	95.60 (34)	
ITR 80015 Green	HC-DRN	700	95.87 (35)	95.76 (36)	95%
TVI 8003 Blue	HC-DRN	1000	95.95 (36)	95.93 (37)	
TVI 80025 Purple	HC-DRN	700	96.45 (37)	96.32 (38)	
XR 8015 (Steel)	FF-STN	200	97.17 (38)	95.72 (35)	
ITR 8002 Yellow	HC-DRN	700	97.19 (39)	97.07 (39)	

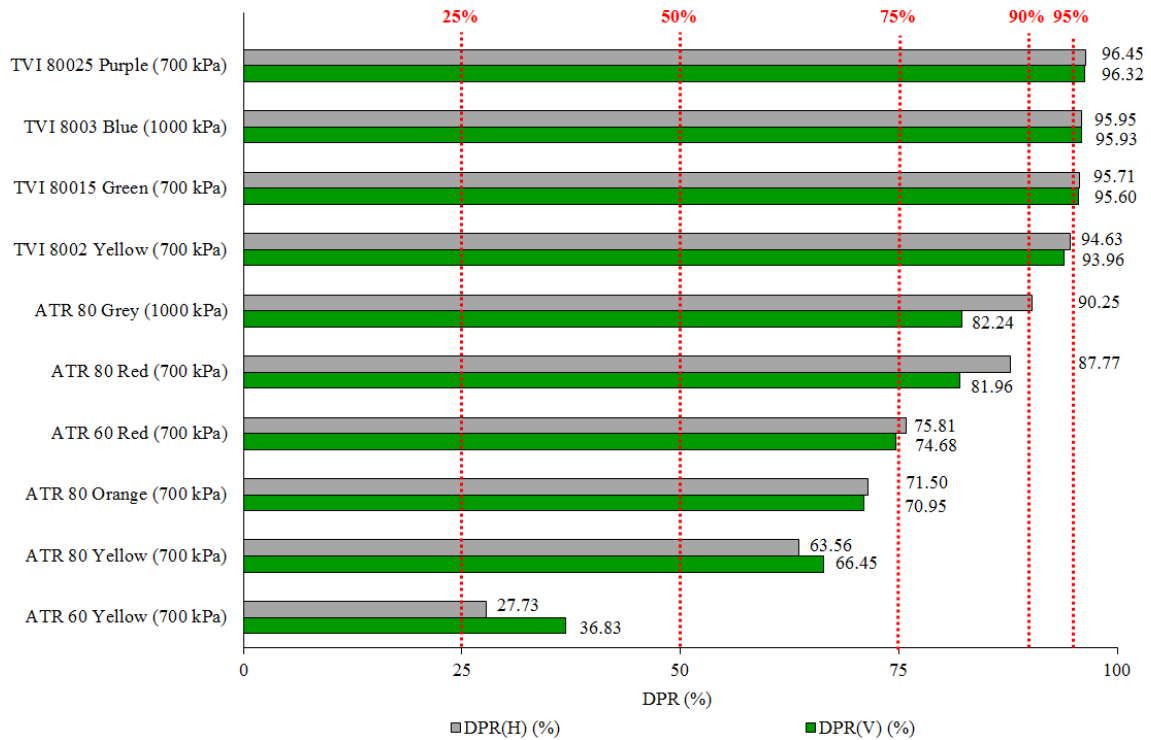
330 <sup>a, b, c, d</sup> Threshold nozzles corresponding to 25%, 50%, 75%, 90% and 95% drift reduction classes, respectively.

331 *HC-STN: Hollow-cone standard nozzle; HC-DRN: Hollow-cone drift reduction nozzle; FC-STN: Full-cone standard nozzle; FF-STN:*

332 *Flat-fan standard nozzle; FF-DRN: Flat-fan drift reduction nozzle.*

333

334 Classification of the Albus nozzles, shown in Fig. 4, is based on the  $DPR_H$  and  $DPR_V$ . The STN  
335 (ATR) nozzles, with the exception of the ATR 80 Grey for the  $DPR_H$  which is at the upper limit,  
336 are below the 90% reduction threshold. In contrast, all the DRN (TVI) nozzles are above this  
337 threshold.



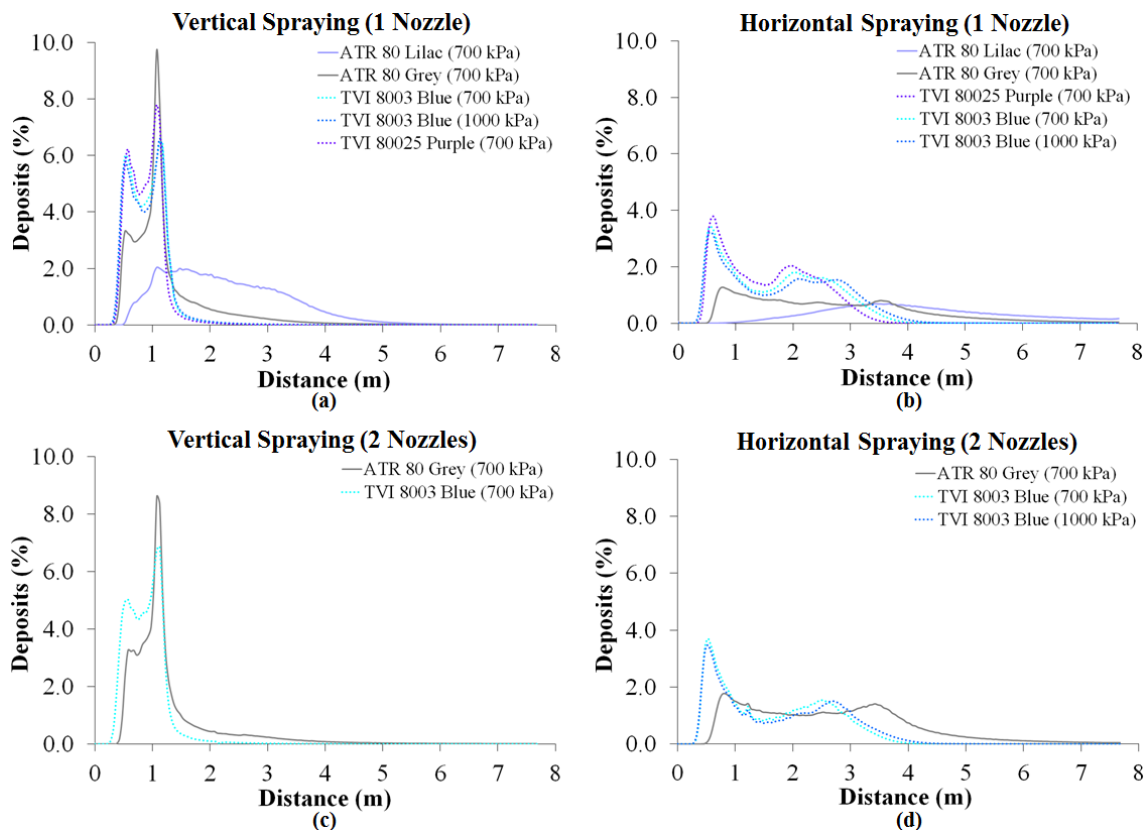
338

339 Fig. 4. Nozzle classification based on  $DPR_H$  and  $DPR_V$  measured with WT1. Reference nozzle: Albus ATR Lilac  
 340 700 kPa.

### 341 3.3. Volumetric wind tunnel (WT2) tests

342 In the WT2 tests, four different spray configurations were studied, with the nozzles oriented  
 343 vertically and horizontally and using in each case one or two nozzles simultaneously. In most of  
 344 the deposition curves (Fig. 5), two peaks can be observed, each corresponding to the two extremes  
 345 of the hollow cone generated by the nozzle. Also apparent is the similarity between the DRN-  
 346 generated curves, with no nozzle size effect observable as also seen in the WT1 tests (Fig. 5). In  
 347 the single-nozzle tests, there are clear differences in the deposition curves generated from the  
 348 vertical (Fig. 5a) and horizontal (Fig. 5b) nozzle positions. In the vertical spray, the deposition  
 349 peaks are higher, though shorter distances are attained of up to 1.5-2 m for the DRN and 4 m for  
 350 the STN nozzles. In contrast, with horizontal spraying, the distances increase to 3-4 m for the  
 351 DRN and 6 m for the STN nozzles, due to the respective droplet sizes. In the double-nozzle tests,  
 352 similar results were obtained, after normalising for the spray flow rate, to those of the single-  
 353 nozzle tests (Fig. 5c, 5d).

354



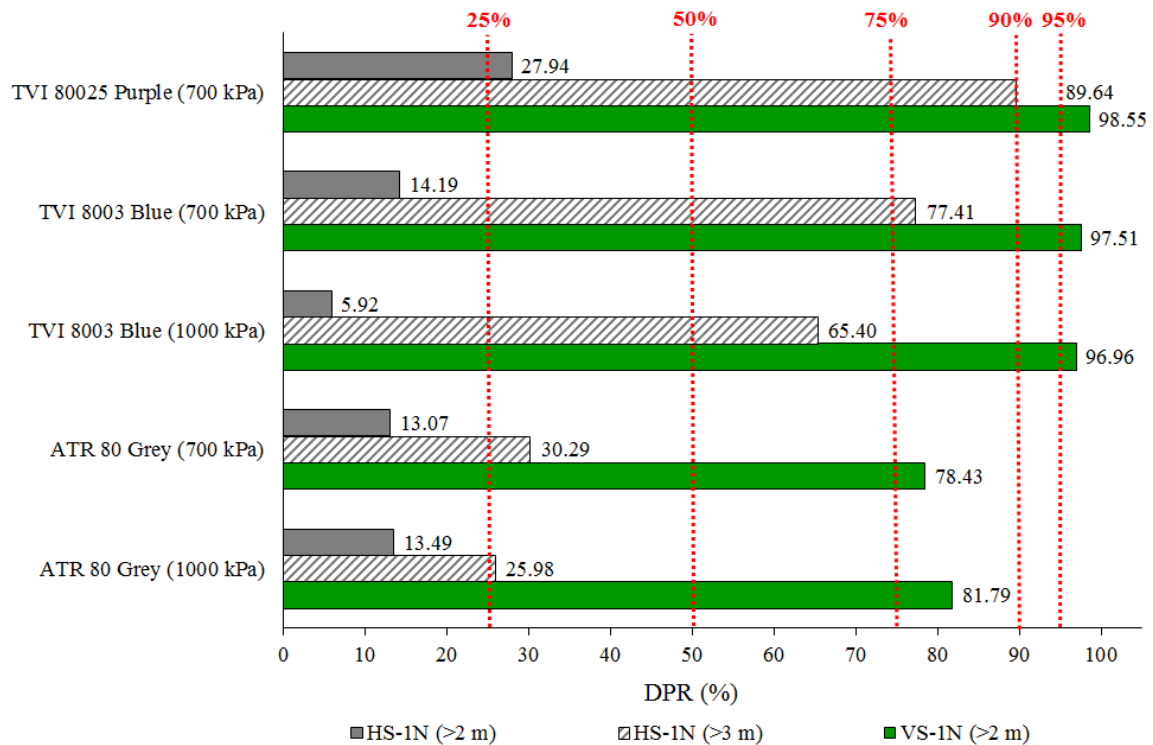
355

356 **Fig. 5.** Deposition curves corresponding to four different spraying arrangements using WT2. (a) Vertical spraying with  
 357 1 nozzle; (b) Horizontal spraying with 1 nozzle; (c) Vertical spraying with 2 nozzles; (d) Horizontal spraying with 2  
 358 nozzles.

359

360 Fig. 6 shows nozzle classification relative to the reference nozzle (ATR Lilac at 700 kPa) based  
 361 on sedimenting drift WT2 measurements. In the vertical configuration, depositions at distances  
 362 from the nozzle beyond 2 m were considered, as proposed in ISO 22856:2008. The  $DPR_H$  values  
 363 enabled differentiation of nozzle type, with the DRN (TVI 80025 Purple and TVI 8003 Blue)  
 364 nozzles situated in the 95% spray drift reduction class, and the STN (ATR 80 Grey) in the 75%  
 365 class. Contrastingly, nozzle type classification was not possible in the horizontal spraying tests,  
 366 with  $DPR_H$  values below 50% obtained in all cases. It was consequently decided to consider only  
 367 depositions beyond 3 m, allowing in this way nozzle type differentiation (STN, DRN). Other

368 interesting result to be underlined is the non-correspondence between the classification of HS-1N  
 369 (>3 m) related to VS-1N (>2 m) and the great capacity of the first one to discriminate classes.



370

371 **Fig. 6.** Nozzle classification based on  $DPR_H$  measured with WT2. HS-1N (>2m) and HS-1N (>3m): a single nozzle  
 372 spraying in horizontal position, considering depositions at distances further than 2 m and 3 m, respectively. VS-1N  
 373 (>2m): a single nozzle spraying in vertical position, considering depositions at distances further than 2 m. Reference  
 374 nozzle: ATR Lilac at 700 kPa.

### 375 3.4. Methods comparison

376 Shown in Table 7 is a comparison of the drift reduction classes established on the basis of the  
 377 parameters evaluated with the PDPA ( $V_{100}$ ,  $V_{200}$ ,  $D_{V50}$ ) and the WT1 (sedimenting and airborne  
 378 depositions), for the 8 hollow-cone nozzle models tested with both methodologies and 2 more  
 379 tested only with the PDPA at a different pressure. Based on the  $DPR$  values determined in sections  
 380 3.1 and 3.2 and in accordance with ISO 22369-1:2006, the following drift reduction classes are  
 381 presented: A ( $\geq 99\%$ ), B ( $95 \leq 99\%$ ), C ( $90 \leq 95\%$ ), D ( $75 \leq 90\%$ ), E ( $50 \leq 75\%$ ) and F ( $25 \leq 50\%$ ).  
 382 Class G is also defined for reductions below 25%.



383 The different models are ordered from highest to lowest  $DPR_{V100}$  value.

384 The other parameters evaluated also followed a decreasing reduction class order. However, two  
 385 exceptions were observed: TVI 8002 Yellow at 700 kPa tested in WT1 ( $DPR_H$  and  $DPR_V$ ) and  
 386 ATR 80 Grey at 1000 kPa also tested in WT1 ( $DPR_H$ ). In the first case, the TVI 8002 Yellow  
 387 nozzle should be in the same drift reduction class as the other DRN models. It can be seen in  
 388 Table 6 that the  $DPR$  values for this nozzle obtained in WT1 are very close to the limit of classes  
 389 B and C, and so, in effect, it could be considered equivalent to the other DRN models. With  
 390 respect to the second exception, ATR 80 Grey, this appears in Table 7 in the position following  
 391 ATR80 Red due to its higher, though very close,  $V_{100}$  value (Table 4). If this nozzle had been  
 392 tested at the same pressure as the other STN models (700 kPa), the respective positions of these  
 393 two nozzles would very probably have been inverted, with which the class C would be justified.  
 394 In fact, the  $DPR_H$  values of both nozzles were very similar and very close to the limit between  
 395 classes C and D (Table 6).

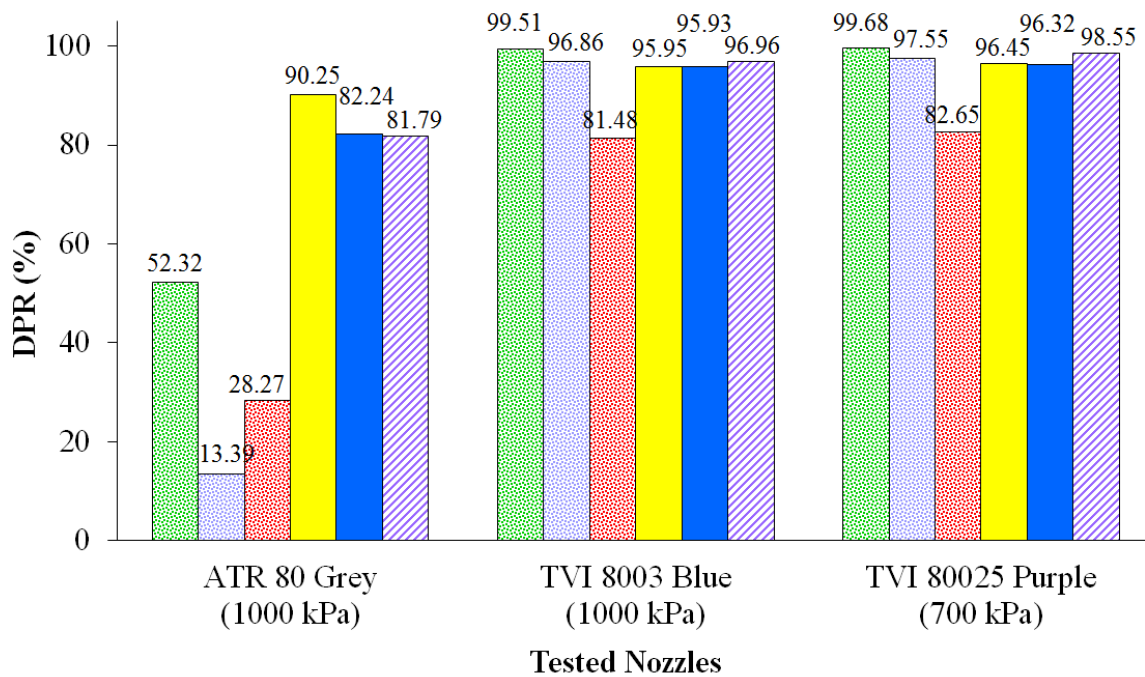
396 **Table 7.** Drift reduction classes determined from PDPA and WT1 evaluated parameters. Classes are defined according  
 397 to the following  $DPR$  values: A ( $\geq 99\%$ ), B ( $95 \leq 99\%$ ), C ( $90 \leq 95\%$ ), D ( $75 \leq 90\%$ ), E ( $50 \leq 75\%$ ), F ( $25 \leq 50\%$ ) and G  
 398 ( $\leq 25\%$ ). Nozzles are sorted by  $DPR_{V100}$ .

Nozzle		Pressure (kPa)	PDPA			WT1	
Model	Type		$DPR_{V100}$ (%)	$DPR_{V200}$ (%)	$DPR_{DV50}$ ( $\mu\text{m}$ )	$DPR_H$ (%)	$DPR_V$ (%)
TVI 80025 Purple	HC-DRN	700	A	B	D	B	B
TVI 8002 Yellow	HC-DRN	700	A	B	D	C	C
TVI 80015 Green	HC-DRN	700	A	B	D	B	B
TVI 8003 Blue	HC-DRN	1000	A	B	D	B	B
TVI 8003 Blue	HC-DRN	700	A	B	D	-	-
ATR 80 Grey	HC-STN	700	E	G	F	-	-
ATR 80 Red	HC-STN	700	E	G	F	D	D
ATR 80 Grey	HC-STN	1000	E	G	F	C	D
ATR 80 Orange	HC-STN	700	F	G	G	E	E
ATR 80 Yellow	HC-STN	700	F	G	G	E	E

399 *HC-STN: Hollow-cone standard nozzle; HC-DRN: Hollow-cone drift reduction nozzle.*

400

401 A comparison is shown in Fig. 7 of the *DPR* of the three nozzle models (ATR 80 Grey at 1000  
 402 kPa, TVI 8003 Blue at 1000 kPa, and TVI 80025 Purple at 700 kPa) which were evaluated with  
 403 all three methodologies used in this study. For each methodology, the *DPR* is expressed  
 404 considering the following parameters: PDPA ( $D_{v50}$ ,  $V_{100}$  and  $V_{200}$ ), WT1 (sedimenting and  
 405 airborne deposition), and WT2 (sedimenting deposition with vertically positioned nozzle).  
 406 The *DPR* values of WT2 (V-1N) are comparable to those obtained in WT1, both for the STN  
 407 model and the two DRN models. For the set of 3 nozzles, the same considerations can also be  
 408 maintained as established for Table 7, with values of different order of magnitude observed  
 409 between WT and PDPA for the STN model and of the same order for the DRN models.  
 410



411 ■ V100    ■ V200    ■ Dv50    ■ WT1 (H)    ■ WT1 (V)    ■ WT2 (SV-1N)

412 **Fig. 7.** Comparison between *DPR* values based on the following parameters: PDPA ( $D_{v50}$ ,  $V_{100}$  and  $V_{200}$ ), WT1 (V and  
 413 H) and WT2 (SV-1N). Reference nozzle: ATR 80 Lilac at 700 kPa.

414 In order to identify the characteristic parameter of the droplet size spectrum which best fits the  
 415 results obtained with WT1, 6 simple linear regressions were performed. In these regressions, the  
 416 *DPR* values calculated using PDPA ( $DPR_{V100}$ ,  $DPR_{V200}$  and  $DPR_{Dv50}$ ) and those obtained with  
 417 WT1 ( $DPR_H$  and  $DPR_V$ ) were correlated for the hollow-cone nozzles common to both

418 methodologies (STN: ATR 80 Yellow, Orange and Red at 700 kPa, ATR 80 Grey at 1000 kPa;  
419 and DRN: TVI 8002 Yellow, 80015 Green, 80025 Purple at 700 kPa and TVI 8003 Blue at 1000  
420 kPa).

421 The results of this study revealed that the characteristic parameter which best fits the *DPR*  
422 obtained with WT1 was the  $V_{100}$ , with coefficients of determination  $R^2=0.771$  and  $R^2=0.948$   
423 corresponding to the  $DPR_H-DPR_{V100}$  and  $DPR_V-DPR_{V100}$  correlations, respectively. This was  
424 followed by the  $D_{V50}$  ( $R^2=0.674$  and  $R^2=0.895$ , respectively) and  $V_{200}$  ( $R^2=0.612$  and  $R^2=0.854$ ,  
425 respectively).

#### 426 4. Discussion

427 The droplet size measured for the hollow-cone nozzles using a PDPA showed that DRN nozzles  
428 produced larger droplets than the STN nozzles. This effect has been observed in previous research  
429 on flat-fan nozzles (Nuyttens et al., 2007; Guler et al., 2007). These results were compared with  
430 those reported by van de Zande et al. (2008), and it was seen that the  $D_{V10}$ ,  $D_{V50}$  and  $D_{V90}$  values  
431 obtained in our study were lower for the STN and higher for the DRN nozzles. With respect to  
432 the  $V_{100}$  and  $V_{200}$  parameters, in our study higher values were obtained for the STN and lower  
433 values for the DRN nozzles. The differences between the results obtained in these two laboratories  
434 can be attributed to the characteristics and calibration of the equipment used and the actual nozzle  
435 units employed, as was previously indicated by Nuyttens (2007). Regarding the nozzle  
436 classification based on DPR values (Table 5), the  $DPR_{V100}$  and  $DPR_{V200}$  allow a similar  
437 classification only for DRN nozzles, while the  $DPR_{DV50}$  classifies in a different way all types of  
438 nozzles.

439 Regarding the nozzle size, for the STN nozzles, the  $V_{100}$  value decreased when nozzle size  
440 increased and significant differences between different sizes were observed. For DRN nozzles,  
441 no significant differences were obtained. In flat-fan nozzles, Nuyttens et al. (2009) also observed  
442 the importance of the effect of nozzle type (STN and DRN) and that the effect of nozzle size was  
443 more important in the case of STN than DRN nozzles.

444 For both type of nozzles (STN and DRN) evaluated in WT1, equivalent  $DPR_H$  and  $DPR_V$  values  
445 were observed, obtaining similar classification for each nozzle. This similarity between  
446 sedimenting and airborne deposition results was also observed in FF-type nozzles tested by Taylor  
447 et al. (2004). However, for the risk assessment both measurements must be taken into account. In  
448 general, the DPR of the STN models (ATR 80 Yellow, Orange, Red and Grey) increases with  
449 nozzle size, as expected. In contrast, this behaviour has not been observed for DRN nozzles.

450 In WT2 vertical and horizontal nozzle positions were studied. In the case of vertical spraying, the  
451 deposition did not reach the final section of the tunnel (Fig. 5a). For nozzle classification in the  
452 horizontal configuration (Fig. 6) is preferable to consider depositions at distances further than 3  
453 m instead of 2 m to avoid misinterpretations (e.g., parabolic droplet path). Moreover, in order to  
454 reduce the testing time, two nozzles could be used (Fig. 5c,d), as the deposition collected in both  
455 cases was almost proportional to the sprayed volume.

456 Methods comparison shows that the wind tunnel WT1 presents less capacity to discriminate  
457 between nozzle types (DRN, STN) than the PDPA (Table 7). This may be explained by the  
458 interaction of other factors in the tunnel other than droplet size (e.g. air-droplet fluid dynamics,  
459 which can be variable). Regarding the correlation between  $DPR$  values based on PDPA and WT1  
460 measurements, the  $V_{100}$  was the best indicator of sedimenting ( $R^2=0.771$ ) and airborne ( $R^2=0.948$ )  
461 deposition. The results showed that both wind tunnels (WT1 and WT2) classify in a similar way  
462 (Fig. 7) despite the different nozzle position (vertical and horizontal in WT1 and WT2,  
463 respectively).

464 To establish consistent comparisons between assessment methods it would be necessary to  
465 dispose of wider results with additional nozzle types. The results presented have been obtained  
466 by applying indirect methods under controlled conditions. However, in order to determine which  
467 of these methods best approaches the reality, the results obtained in this work should be contrasted  
468 with field drift measurements.

469

## 470 5. Conclusions

471 Different hollow-cone nozzle models were classified according to their drift potential reduction  
472 (*DPR*) using three indirect methods: PDPA, ISO wind tunnel (WT1), and volumetric wind tunnel  
473 (WT2). To the authors' knowledge, this is the first undertaken classification of hollow-cone  
474 nozzles with a wind tunnel, following ISO 22856:2008. The three indirect methods have shown  
475 that the DRN nozzles have *DPR* values greater than 90% in comparison with the STN. The use  
476 of this type of nozzles should be promoted with the aim of reducing the bystanders and residents'  
477 exposure, and the environment contamination.

478 The findings of this work show that an equally valid initial hollow-cone nozzle classification can  
479 be obtained with either the  $V_{100}$  or the  $DPR_v$ . Compared to the wind tunnel, the PDPA allows a  
480 simplified and faster classification methodology. However, the wind tunnel cannot be overlooked  
481 when trying to evaluate sedimenting drift ( $DPR_H$ ) for risk prevention of surface waters, soils and  
482 non-target areas in general.

483 The WT2 results point to the horizontal position of the tested nozzle as an interesting methodology  
484 for testing hollow-cone nozzles. Further studies are required to establish a new indirect  
485 methodology to classify cone nozzles, where the test conditions can be approximated to real  
486 working conditions in the field (droplet orientation and air-assistance).

487 Progress should be made in the development of new simplified methods for nozzle assessment  
488 under real operation conditions, an issue that is addressed in Part 2 of this work. Further studies  
489 are needed for a global evaluation of hollow-cone DRN. Neither the beneficial effect for  
490 environment and human risk mitigation nor the efficacy of the DRN have not yet been assessed.  
491 Finally, it should be verified that the balance of DRN in terms of environmental and efficacy  
492 against pests is favorable.

## 493 Acknowledgements

494 This work was partly funded by the Secretaria d'Universitats i Recerca del Departament  
495 d'Empresa i Coneixement de la Generalitat de Catalunya, the Spanish Ministry of Economy and  
496 Competitiveness and the European Regional Development Fund (ERDF) under Grants 2017 SGR  
497 646, AGL2007-66093-C04-03, AGL2010-22304-04-C03-03, and AGL2013-48297-C2-2-R. The  
498 authors also wish to thank Mr. Antonio Checa (Randex Iberica, S.L.) for giving us free Albuz  
499 nozzles for the spray tests. Universitat de Lleida is also thanked for Mr. X. Torrent's pre-doctoral  
500 fellowship.

501

## 502 **References**

503 Arvidsson, T., Bergstrom, L., Kreuger, J., 2011. Spray drift as influenced by meteorological and  
504 technical factors. *Pest Manage. Sci.* 67, 586–598. <https://doi.org/10.1002/ps.2114>.

505 Balsari, P., Marucco, P., Tamagnone, M., 2007. A test bench for the classification of boom  
506 sprayers according to drift risk. *Crop Prot.* 26, 1482–1489.  
507 <https://doi.org/10.1016/j.cropro.2006.12.012>.

508 Bouse, L.F., Kirk, I.W., Bode, L.E., 1990. Effect of spray mixture on droplet size. *Trans. ASAE*  
509 33 (3): 783-788.

510 Butler Ellis, M.C., Alanis, R., Lane, A.G., Tuck, C.R., Nuyttens, D., van de Zande, J.C., 2017.  
511 Wind tunnel measurements and model predictions for estimating spray drift reduction under  
512 field conditions. *Biosyst. Eng.* 154, 25-34

513 Butler Ellis, M.C., Kennedy, M.C., Kuster, C.J., Alanis, R., Tuck, C.R., 2018. Improvements in  
514 modelling bystander and resident exposure to pesticide spray drift: Investigations into new  
515 approaches for characterizing the 'collection efficiency' of the human body. *Ann. Work*  
516 *Expos. Health* 62(5), 622-632. <http://dx.doi.org/10.1093/annweh/wxy017>.

517 Butler Ellis, M.C., Lane, A.G., O'Sullivan, C.M., Miller, P.C.H., Glass, C.R., 2010. Bystander  
518 exposure to pesticide spray drift: new data for model development and validation. *Biosyst.*

- 519 Eng. 107, 162-168.
- 520 Damalas, Christos A. 2015. Chapter 15. Pesticide drift: seeking reliable environmental indicators  
521 of exposure assessment. In Armon RH, Hanninen O (Eds) Environmental Indicators.  
522 Springer Publishing Company, the Netheralnds, pp. 251-264.
- 523 Derksen, R.C., Ozkan, H.E., Foz, R.D., Brazee, R.D., 1999. Droplet spectrum and wind tunnel  
524 evaluation of Venturi and pre-orifice nozzles. T. ASAE 42 (6), 1573-1580.
- 525 Douzals, J.P., Al Heidary, M. 2014. How spray characteristics and orientation may influence  
526 spray drift in a wind tunnel. Asp. Appl. Biol.122, International Advances in Pesticide  
527 Application, pp. 271-279.
- 528 Douzals, J.P., Al Heidary, M., Sinfort, C., 2016. Spray deposition in a wind tunnel: a kinetic  
529 approach of the wind speed effects. Asp. Appl. Biol. 132, International Advances in  
530 Pesticide Application, pp. 299-309.
- 531 Douzals, J.P., Al Heidary, M., Sinfort, C., 2018. In situ droplet size measurements in a wind  
532 tunnel. Asp. Appl. Biol. 137, International Advances in Pesticide Applications, pp. 237-244.
- 533 Ferguson, J.C., Chechetto, R.G., O'Donnell, C.C., Dorr, G.J., Moore, J.H., Baker, G.J., Powis,  
534 K.J., Hewitt, A.J., 2016. Determining the drift potential of venturi nozzles compared with  
535 standard nozzles across three insecticide spray solutions in a wind tunnel. Pest. Manag. Sci.  
536 72, 1460-1466. <http://dx.doi.org/10.1002/ps.4214>.
- 537 Ferguson, J.C., O'Donnell, C.C., Chauhan, B.S., Adkins, S.W., Kruger, G.R., Wang, R., Ferreira,  
538 P.H.U., Hewitt, A.J., 2015. Determining the uniformity and consistency of droplet size  
539 across spray drift reducing nozzles in a wind tunnel. Crop Prot. 76, 1-6.  
540 <http://dx.doi.org/10.1016/j.cropro.2015.06.008>.
- 541 Garcerá, C., Moltó, E., Chueca, P., 2017. Spray pesticide applications in Mediterranean citrus  
542 orchards: Canopy deposition and off-target losses. Sci. Total Environ. 599-600, 1344-1362.  
543 <http://dx.doi.org/10.1016/j.scitotenv.2017.05.029>.

- 544 Gil, E., Balsari, P., Gallart, M., Llorens, J., Marucco, P., Andersen, P.G., Fàbregas, X., Llop, J.,  
545 2014. Determination of drift potential of different flat fan nozzles on a boom sprayer using  
546 a test bench. *Crop Prot.* 56, 58–68. <https://doi.org/10.1016/j.cropro.2013.10.018>.
- 547 Gregorio, E., Rosell-Polo, J.R., Sanz, R., Rocadenbosch, F., Solanelles, F., Garcerà, C., Chueca,  
548 P., Arnó, J., del Moral, I., Masip, J., Camp, F., Viana, R., Escolà, A., Gràcia, F., Planas, S.,  
549 Moltó, E., 2014. LIDAR as an alternative to passive collectors to measure pesticide spray  
550 drift. *Atmos. Environ.* 82, 83–93. <http://dx.doi.org/10.1016/j.atmosenv.2013.09.028>.
- 551 Gregorio, E., Torrent, X., Planas, S., Solanelles, F., Sanz, R., Rocadenbosch, F., Masip, J., Ribes-  
552 Dasi, M., Rosell-Polo, J.R., 2016. Measurement of spray drift with a specifically designed  
553 lidar system. *Sensors (Switzerland)* 16. <https://doi.org/10.3390/s16040499>.
- 554 Gregorio, E., Torrent, X., Planas, S., Rosell-Polo, J.R., 2019. Assessment of spray drift for  
555 hollow-cone nozzles: Part 2. Lidar technique (Submitted for publication).
- 556 Grella, M., Marucco, P., Balsari, P., 2019. Toward a new method to classify the airblast sprayers  
557 according to their potential drift reduction: comparison of direct and new indirect  
558 measurement method. *Pest Manag. Sci.* (in press). <https://doi.org/10.1002/ps.5354>.
- 559 Guler, H., Zhu, H., Ozkan, H.E., Derksen, R.C., Krause, C.R., 2006. Wind tunnel evaluation of  
560 drift reduction potential and spray characteristics with drift retardants at high operating  
561 pressure. *Journal of ASTM International*, 3 (5). Paper ID JAI13527.
- 562 Guler, H., Zhu, H., Ozkan, H.E., Derksen, R.C., Yu, Y., Krause, C.R., 2007. Spray characteristics  
563 and drift reduction potential with air induction and conventional flat-fan nozzles. *Trans.*  
564 *ASABE* 50 (3), 745-754.
- 565 Herbst, A., 2001a. A method to determine spray drift potential from nozzles and its links to buffer  
566 zone restrictions. In: *ASAE Annual International Meeting*. USA, Sacramento.
- 567 Herbst, A., 2001b. Droplet sizing on agricultural sprays-A comparison of measuring systems  
568 using a standard droplet size classification scheme. In: *Proceedings Ilass Europe 2001*.



- 569 Switzerland, Zurich.
- 570 Hiscox, A.L., Miller, D.R., Nappo, C.J., Ross, J., 2006. Dispersion of Fine Spray from Aerial  
571 Applications in Stable Atmospheric Conditions. *Trans. ASABE* 49, 1513–1520.
- 572 Holterman, H.J., 2008. Effects of PDA sampling techniques on spectruml characteristics of  
573 agricultural sprays. WUR Plant Research International. P.O. Box 16, 6700 AA.  
574 Wageningen.
- 575 Holterman, H.J., 2009. Comparison of 1D PDA sampling methods to obtain drop size and velocity  
576 distributions inside a spray cone of agricultural nozzles. WUR Plant Research International.  
577 P.O. Box 616, 6700 AP. Wageningen.
- 578 Holterman, H.J., van de Zande, J.C., Huijsmans, J.F.M., Wenneker, M., 2017. An empirical model  
579 based on phenological growth stage for predicting pesticide spray drift in pome fruit  
580 orchards. *Biosyst. Eng.* 154, 46-61. <http://dx.doi.org/10.1016/j.biosystemseng.2016.08.016>.
- 581 ISO 22369-1, 2006. Crop protection equipment - Drift classification of spraying equipment - Part  
582 1: Classes. International Organization for Standardization, Geneva.
- 583 ISO 22856, 2008. Equipment for crop protection - Methods for the laboratory measurement of  
584 spray drift - Wind tunnels. International Organization for Standardization, Geneva.
- 585 ISO 22866, 2005. Equipment for crop protection - Methods for field measurement of spray drift.  
586 International Organization for Standardization, Geneva.
- 587 ISO 25358, 2018. Crop protection equipment - Droplet-size spectra from atomizers -  
588 Measurement and classification. International Organization for Standardization, Geneva.
- 589 Kashdan, J.T., Shrimpton, J.S., Whybrew, A., 2007. A digital image analysis technique for  
590 quantitative characterization of high-speed sprays. *Opt. Lasers Eng.* 45, 106– 115.
- 591 Kasner, E.J., Fenske, R.A., Hoheisel, G.A., Galvin, K., Blanco, M.N., Seto, E.Y.W., Yost, M.G.,  
592 2018. Spray drift from a conventional axial fan airblast sprayer in a modern Orchard work

- 593 environment. *Ann. Work Expo. Health* 62, 1134-1146.  
594 <https://doi.org/10.1093/annweh/wxy082>.
- 595 McCartney, S.J., Obermiller, J.D., 2008. Comparative performance of air-induction and  
596 conventional nozzles on an axial fan sprayer in medium density apple orchards.  
597 *Hortechology* 18 (3), 365-371.
- 598 Miranda-Fuentes, A., Marucco, P., González-Sánchez, E.J., Gil, E., Grella, M., Balsari, P., 2018.  
599 Developing strategies to reduce spray drift in pneumatic spraying in vineyards: Assessment  
600 of the parameters affecting droplet size in pneumatic spraying. *Sci. Total. Environ.* 616-617,  
601 805-815. <https://doi.org/10.1016/j.scitotenv.2017.10.242>.
- 602 Nuyttens, D., 2007. Drift from field crop sprayers: The influence of spray application technology  
603 determined using indirect and direct drift assessment means. PhD thesis nr. 772, KU Leuven.  
604 293 p. ISBN 978-908826-039-1. Katholieke Universiteit Leuven - Faculteit Bio-  
605 ingenieurswetenschappen. <https://doi.org/10.1017/CBO9781107415324.004>.
- 606 Nuyttens, D., Baetens, K., De Schampheleire, M., Sonck, B., 2007. Effect of nozzle type, size and  
607 pressure on spray droplet characteristics. *Biosyst. Eng.* 97, 333-345.  
608 <https://doi.org/10.1016/j.biosystemseng.2007.03.001>.
- 609 Nuyttens, D., Taylor, W.A., Schampheleire, M. De, Verboven, P., Dekeyser, D., 2009. Influence  
610 of nozzle type and size on drift potential by means of different wind tunnel evaluation  
611 methods. *Biosyst. Eng.* 103, 271-280.  
612 <https://doi.org/10.1016/j.biosystemseng.2009.04.001>.
- 613 Taylor, W.A., Womac, A.R., Miller, P.C.H., Taylor, B.P., 2004. An Attempt to Relate Drop Size  
614 to Drift Risk. In: *International Conference on Pesticide Application for Drift Management*  
615 *Octobre 27-29.* pp. 210-223.
- 616 Teske, M.E., Thistle, H.W., Mickle, R.E., 2000. Modeling finer droplet aerial spray drift and  
617 deposition. *Appl. Eng. Agric.* 16, 351-357.

- 618 Torrent, X., Garcerá, C., Moltó, E., Chueca, P., Abad, R., Grafulla, C., Román, C., Planas, S.,  
619 2017. Comparison between standard and drift reducing nozzles for pesticide application in  
620 citrus: Part I. Effects on wind tunnel and field spray drift. *Crop Prot.* 96, 130–143.  
621 <https://doi.org/10.1016/j.cropro.2017.02.001>.
- 622 Tuck, C.R., Butler-Ellis, M.C., Miller, P.C.H., 1997. Techniques for measurement of droplet size  
623 and velocity distributions in agricultural sprays. *Crop Prot.* 16, 619-628.
- 624 Van de Zande, J.C., Holterman, H.J., Wenneker, M., 2008. Nozzle classification for drift  
625 reduction in orchard spraying: Identification of drift reduction class threshold nozzles.  
626 *Agricultural Engineering International: the CIGR Ejournal*. Manuscript ALNARP 08 0013.  
627 Vol. X.